SCIEPublish

Article

Transparent, Hydrolysable and Flame Retarded Bio-based Epoxy Resins via Catalyst-free Polymerization of Triglycidyl Isocyanurate and Aliphatic Diacids

Tianlong Ma [1], Donglin Tang [1,2,*]

[1] Department of Polymer Materials Science Engineering, South China University of Technology, Guangzhou 510640, China; msmatianlong@mail.scut.edu.cn (T.M.)

[2] Guangdong Provincial Key Laboratory of Luminescence from Molecular Aggregates, South China University of Technology, Guangzhou 510640, China

* Corresponding author. E-mail: msdltang@scut.edu.cn (D.T.)

Received: 24 March 2023; Accepted: 26 May 2023; Available online: 1 June 2023

ABSTRACT: In this study, transparent and hydrolysable intrinsic flame retarded epoxy resins were synthesized successfully by melting polymerization without any catalyst, simply from bio-based triglycidyl isocyanurate and aliphatic diacids. Due to the possibility of transesterification along with the ring-opening reaction, the most suitable feed ratio of [COOH]/[epoxy] is found to be 60%. By changing the carbon number of diacid from 8 to 12, ER08-60, ER10-60 and ER12-60 were synthesized. The flame retardancy of ER08-60 is found to be excellent, with a UL-94 rating at V-0 and a LOI value at 27.6%. It is revealed from this study that upon heating isocyanurate ring decomposes first and CO_2 released prevents the contact of materials with oxygen, thus preventing further combustion. The tensile strength and bending strength of ER08-60 can reach 86.6 MPa and 75.4 MPa, respectively. Additionally, all epoxy resins are able to hydrolyze quickly in both acid and alkaline solutions. It is worth to mention that these epoxy resins are transparent, with a transmittance of around 85%.

Keywords: Bio-based epoxy resins; Intrinsic flame retardancy; Isocyanurate ring; Hydrolysable

1. Introduction

Epoxy resins (ERs) are widely used in transportation, construction, electronics, machinery and other fields due to their excellent mechanical properties, bonding properties, chemical stability and dimensional stability [1–5]. However, current commercial ERs are flammable, restricting their further applications in fields where fire resistance is required, e.g., in the construction field. Therefore, the development of flame retarded, especially intrinsic flame retarded ERs are in the interests of many researchers [6–8].

Nowadays, most of ERs are made from petroleum-based diglycidyl ether bisphenol A. Since the petroleum resources are limited and the petroleum price is drastically fluctuating due to the unstable political issues, bio-based ERs based on renewable biomass resources are considered to be more sustainable and they have attracted more attention of researchers and manufacturers [6,7,9–11].

To induce flame retardancy into bio-based ERs, one efficient and conventional way is directly adding flame retardants in the curing process [8,12]. However, there is some negative influence in this case, such as poor compatibility between ERs and flame retardant additives, migration of additives from ERs, etc. One of the solutions is to introduce flame retardant segments containing P [13–15], N [16–19], Si [4] or other flame retarded elements [5,20,21] into the backbones or side groups in bio-based ERs. Tailoring compounds with (poly)aromatic structure from biomass to the structure of epoxy building blocks can also improve the flame retardancy of ERs [11,16,22].

Previous studies have verified that isocyanurate ring structure is able to offer flame retarded function to the formed polymer materials [17,23–25]. Isocyanurate rings can be formed by trimerization of isocyanate [16,25], but the process is not convenient and special catalysts are needed. Another way to form isocyanurate is to apply urea trimerization pyrolysis to synthesize isocyanuric acid (ICA). Due to the certain reactivity of ICA, lots of derivatives bearing reactive functions can be obtained [26], for instance,

https://doi.org/10.35534/spe.2023.10008

triglycidyl isocyanurate (TGIC), tri(2-hydroxyethyl) isocyanurate (THEIC), tri(2-carboxyethyl) isocyanurate (TCEIC), bis(2-carboxyethyl) isocyanurate (BCEIC), etc. In our previous study [19], linear polyisocyanuratoester (PICE) has been prepared from BCEIC and diols. Those PICEs are proved to be flame retarded but it is remains to be an issue that the mechanical properties are not satisfactory. Another way to synthesize polyester could be utilizing the reaction between epoxides and acids. Epoxide, e.g., TGIC, is able to react with amines, alcohols, thiols, anhydrides, acids, etc. TGIC melts at high temperature (above 100 °C), and in this case, the curing reaction would be too fast at melting when amines or thiols are used as the curing agent, due to the high reactivity. The reactivity between acid and epoxide is much lower so that it is possible to perform the melting polymerization of aliphatic diacid (DA) and TGIC. In order to improve the toughness of ERs, DAs with the flexible longer carbon chain would be more preferable [27–29].

In this study, it was proposed to prepare hydrolysable and intrinsic flame retarded ERs based on TGIC and DAs, via an economical and green way. TGIC bearing isocyanurate structure was applied to offer the flame retardancy for the obtained ERs. The introduction of flexible carbon chain was aiming at improving the mechanical properties and the generated ester group made the material hydrolysable. The effects of the feed ratio [TGIC]/[DA] and the chain length of DAs on the properties of ERs were studied. The mechanism of flame retardancy of such isocyanurate-containing ERs was investigated as well.

2. Experimental Section

2.1. Materials

Triglycidyl isocyanurate (TGIC, 99%), 1,12-dodecanedioic acid (DA12, 99%), sebacic acid (DA10, 98%), suberic acid (DA08, 99%) were purchased from Aladdin Biochemical Technology Co. Ltd. (Shanghai, China). Hydrochloric acid (AR) and sodium hydroxide (AR) were supplied by Guangzhou Chemical Reagent Factory (Guangzhou, China).

2.2. Preparation of ERs

The ERs were prepared by melting polymerization. Taking the preparation of ER12-100 as an example, TGIC (5.94 g, 20 mmol) and DA12 (6.91 g, 30 mmol) were added into a vessel and stirred to melt at 130 °C. The molten mixture was kept at 130 °C for 15 min and then poured into a silicon mold, followed by degassing under vacuum at 130 °C. The post-curing reaction was performed in an oven at 130 °C for 12 h. ER12-100 samples with certain dimensions were obtained after removal from the mold.

2.3 Characterizations

The Fourier transform infrared (FT-IR) spectra were recorded on a VERTEX 70 infrared spectrometer (Bruker, Ettlingen, Germany), scanning for 32 times from 400 to 4000 cm^{-1}. Each sample for FT-IR test was prepared by grinding 1 mg polymer together with 150 mg KBr, followed by pelleting. Differential scanning calorimetry (DSC) was performed using a DSC 204 F1 (Netzsch, Selb, Germany) instrument at a heating rate of 20 °C/min and a cooling rate of 10 °C/min under N_2 atmosphere at a flow rate of 40 mL/min. The sample amount for DSC measurements is 2–5 mg. Thermal gravimetric analysis (TGA) was conducted on a TG 209 F1 (Netzsch, Selb, Germany) instrument and the temperature was set to be from room temperature to 800 °C at a heating rate of 10 °C/min in a N_2 atmosphere at a flow rate of 20 mL/min. The amount of sample for TGA tests is 5–10 mg. Dynamic mechanical analysis (DMA) was carried out on a DMA Q800 (TA, New Castle, DE, USA) instrument. Sample cut into 20 × 4 × 2 mm^3 was loaded, and the loading mode was selected as Multi Frequency Strain. After preheating at initial temperature for 5 min, 0.1% strain was preapplied to the samples and the test began with an alternating frequency of 1 Hz and with a temperature range of −20–100 °C. T_g value is determined as the intersection temperature of the tangents of the vitreous region and the vitreous transition region in *E'-T* curves. UL-94 vertical burning test was carried out on vertical burning tester (Modisi, Kunshan, China) with a sample size of 125 × 13 × 3 mm^3 regulated by the standard IEC 60695-11-10: 1999. Limiting oxygen index (LOI) tests were performed using JF-3 digital oxygen index analyzer (Jiangning Analysis Instrument Company, Nanjing, China) according to ASTM-D2863 with the sample size at 100 × 10 × 4 mm^3. Cone calorimetry tests were carried out on a Dual Cone Calorimeter (Noselab-ATS, Bovisio Masciago, Italy) instrument, with the sample size of 100 × 100 × 2 mm^3 and the heat flux was set at 50 kW/m^2 according to ISO 5660-1. According to ISO 527-1: 2019, the tensile test was conducted using an Instron 5960 (Instron, USA) tester with a tensile speed of 5 mm/min and the samples were cut by a cutter according to ISO 37 Type 2. While the tensile stress at 0% to 1%, the tensile speed was set as 0.1 mm/min to obtain the Young's modules. The bending strength was tested by Instron 5960 (Instron, Norwood, MA, USA) with the sample size at 100 × 10 × 4 mm^3 and the bending rate was set at 2 mm/min according to ISO 178-2010. Five specimens for each sample were tested to obtain the average values in both tensile and bending tests. Scanning electron microscopy (SEM) was conducted using EV018 (Zeiss, Oberkochen, Germany) and the samples were gold coated before testing. Thermogravimetric analysis-infrared (TG-IR) spectra was recorded on STA 449C/3MFC/G (Netzsch, Selb, Germany) with a temperature range from 40 °C to 800 °C at a ramp rate of 10 °C/min in a N_2 atmosphere. 10–15 mg of sample was taken for TG-IR measurement. The X-ray photoelectron spectroscopy (XPS) was performed with Axis Ultra DLD (Kratos Analytical, Manchester,

UK). UV/Vis spectrophotometry was determined by Cary 60 (Agilent Technologies, Santa Clara, CA, USA) in the range from 400 nm to 800 nm with the sample size at 40 × 40 × 2 mm^3.

3. Results and Discussion

3.1. Synthesis of ERs

ERs based on TGIC and DAs were prepared by melting polymerization, without any catalysts (see Scheme 1). The DAs used in this study were DA12, DA10 and DA08 so that the products were nominated as ER12-xx, ER10-xx and ER08-xx, respectively (xx: the percentage of the feed ratio of [COOH]/[epoxy]). The melting point of TGIC is around 100 °C, while that of DA is around or even above 130 °C. In this case, the reactant mixtures cannot fully melt when the reaction temperature is lower than 130 °C. But if the temperature is higher than 130 °C, the reaction between TGIC and DA runs so fast that there would be no sufficient time for molding. Therefore, the reaction temperature was set at 130 °C. Not only ring-opening reaction but also transesterification takes place in the curing process between TGIC and DAs [29], as shown in Scheme 1. Both hydroxyl and ester groups generate when the carboxyl group reacts with epoxy group (reaction (i)) and the hydroxyl groups obtained are involved in the esterification and etherification (reactions (ii) and (iii)). In this case, the feed ratio of [COOH]/[epoxy] is an important factor that affects the properties (such as flame retardancy, mechanical properties, etc.) of the final products. The feed ratio of [COOH]/[epoxy] was varied (100%, 80%, and 60%) in the series of ER12 and the samples were designated as ER12-100, ER12-80, and ER12-60, respectively (see Table 1). DA12, DA10 and DA08 are able to melt with TGIC at 130 °C to form clear liquid and the ERs obtained after curation are optically transparent (see Figure S1).

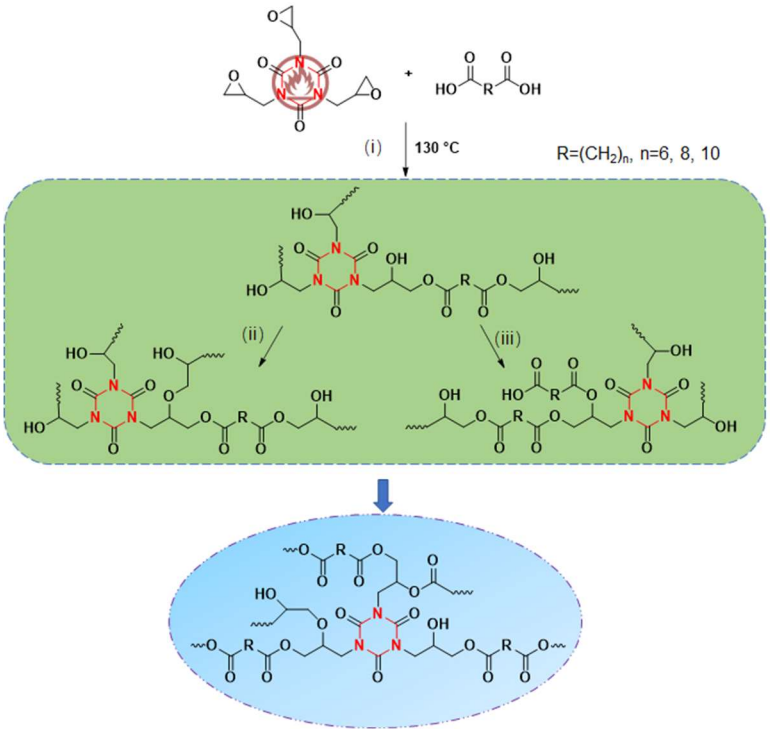

Scheme 1. Synthetic route for ERs based on TGIC and DAs without any catalyst.

Table 1. The reaction conditions and the flame retardancy data of the obtained ERs.

Sample	DA	[COOH]/[ep] (%)	UL-94				LOI (%)
			Rating	t_1/t_2 (s)	Dripping (yes/no)	Cotton Ignition (yes/no)	
ER12-100		100	NR	burn out	no	no	-
ER12-80	DA12	80	NR	burn out	yes	yes	-
ER12-60		60	V-1	29/15	yes	no	23.5
ER10-60	DA10	60	V-1	21/5	yes	no	24.6
ER08-60	DA08	60	V-0	1/1	no	no	27.6

3.2. Effect of Feed Ratio of [COOH]/[epoxy] on the Structure and the Properties of ERs

The FT-IR spectra of the ER12-xx samples with different feed ratio of [COOH]/[epoxy] are shown in Figure 1. The broad absorption band between 3700 and 3200 cm^{-1} was related to formed hydroxyl groups (–OH) and the band at 1740 cm^{-1} was related to the C=O stretching of the obtained ester groups from the ring-opening reaction of epoxy and carboxyl groups and the esterification of hydroxyl and carboxyl groups [29,30]. The two peaks at 2924 and 2852 cm^{-1} corresponded to the asymmetrical and symmetrical C–H stretching of the aliphatic methylene groups while the signal at 1462 cm^{-1} corresponded to the C–N stretching. The peak at 1689 cm^{-1} was related to the C=O stretching signal of isocyanurate group, while the C=O stretching of the ester groups was identified with the absorption peak at 1699 cm^{-1}. The bands between 1242 and 1064 cm^{-1} corresponded to the C–O and C–O–C vibrations of ester, ether, and alcohol, proving the occurrence of esterification. For ER12-60, the peaks at 1689 cm^{-1} and 1646 cm^{-1} were much sharper which is understandable due to the increased amount of isocyanuate segment.

The introduction of isocyanurate ring offers flame retardancy for ERs, and thus the content of isocyanurate ring structure in the obtained ERs determines the flame retardancy. As shown in Table 1, Table S1 and Figure S2, the flame retardancy of ER12-60 is much better than that of ER12-100, ER12-80 and ER12-70. But as the feed ratio of [COOH]/[epoxy] decreased to 0.5, ER12-50 losed flame retardancy. Therefore, the feed ratio of [COOH]/[epoxy] was fixed at 0.6 in the next step of research on the effect of chain length of DAs.

3.3. Effect of Chain Length of DAs on Properties of ERs

Different DAs with different chain length (DA08, DA10 and DA12) were applied to react with TGIC with the same feed ratio of [COOH]/[epoxy] at 0.6 in the synthesis of ERs, and the products were nominated as ER08-60, ER10-60 and ER12-60, respectively.

The TGA and DTG curves of the obtained ERs are shown in Figure 2 and the detailed data are summarized in Table 2. The initial decomposition temperatures ($T_{d,5\%}$) of all the samples were similarly around 270 °C, indicating that these ERs have similar initial thermal stability, regardless of the chain length of DAs. The decomposition of ERs follows a three-stage process, including the decomposition of isocyanurate ring at 300 °C, the pyrolysis of carbon chains and eventually the pyrolysis of carbon residue. The higher second-step decomposition temperature for ER12-60 is understandable due to the longer methylene group [18,31]. As shown in Figure 2c and Table 2, the glass transition temperature (T_g) of ERs increases with the shortening of chain length of DAs, from 45.1 °C for ER12-60 to 64.1 °C for ER08-60. The movement of the network segments is more restricted when the chain length is shorter, resulting in a higher value of T_g. Dynamic thermomechanical properties of ERs were studied via DMA and the curves are shown in Figure 2d. The storage modulus at 30 °C [E' (30 °C)] of ER12-60 and ER10-60 were 1728 and 1790 MPa, while that of ER08-60 improved greatly to 3389 MPa with the decline of chain length of DA. This means that ERs performs well in normal temperature ranges. Moreover, similarly to the DSC results, there was a considerable increase in T_g value determined by the tangent method, along with the decrease of chain length of DA.

Table 2. Thermal properties of the obtained ERs.

Sample	$T_{d,5\%}$ (°C)	$T_{d,max}$ (°C)	T_g (DSC^{1st}) (°C)	T_g (DSC^{2nd}) (°C)	T_g (DMA) (°C)	E' (30 °C) (MPa)
ER12-60	274.5	402.2	49.2	45.1	37.1	1728
ER10-60	266.6	300.8	56.7	50.2	38.2	1790
ER08-60	265.8	304.8	69.6	64.1	59.5	3389

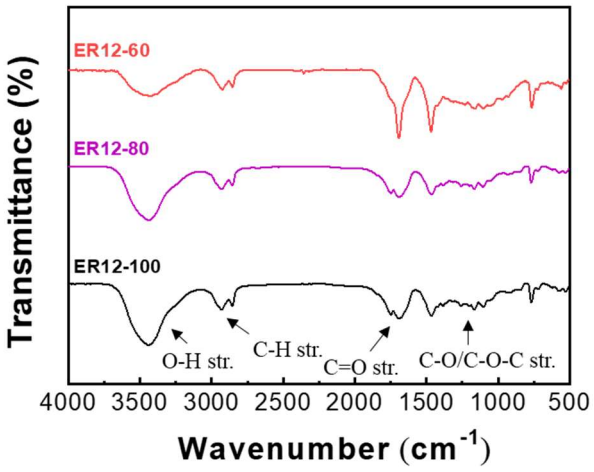

Figure 1. FT-IR spectra of ER12 with different feed ratio of [COOH]/[epoxy].

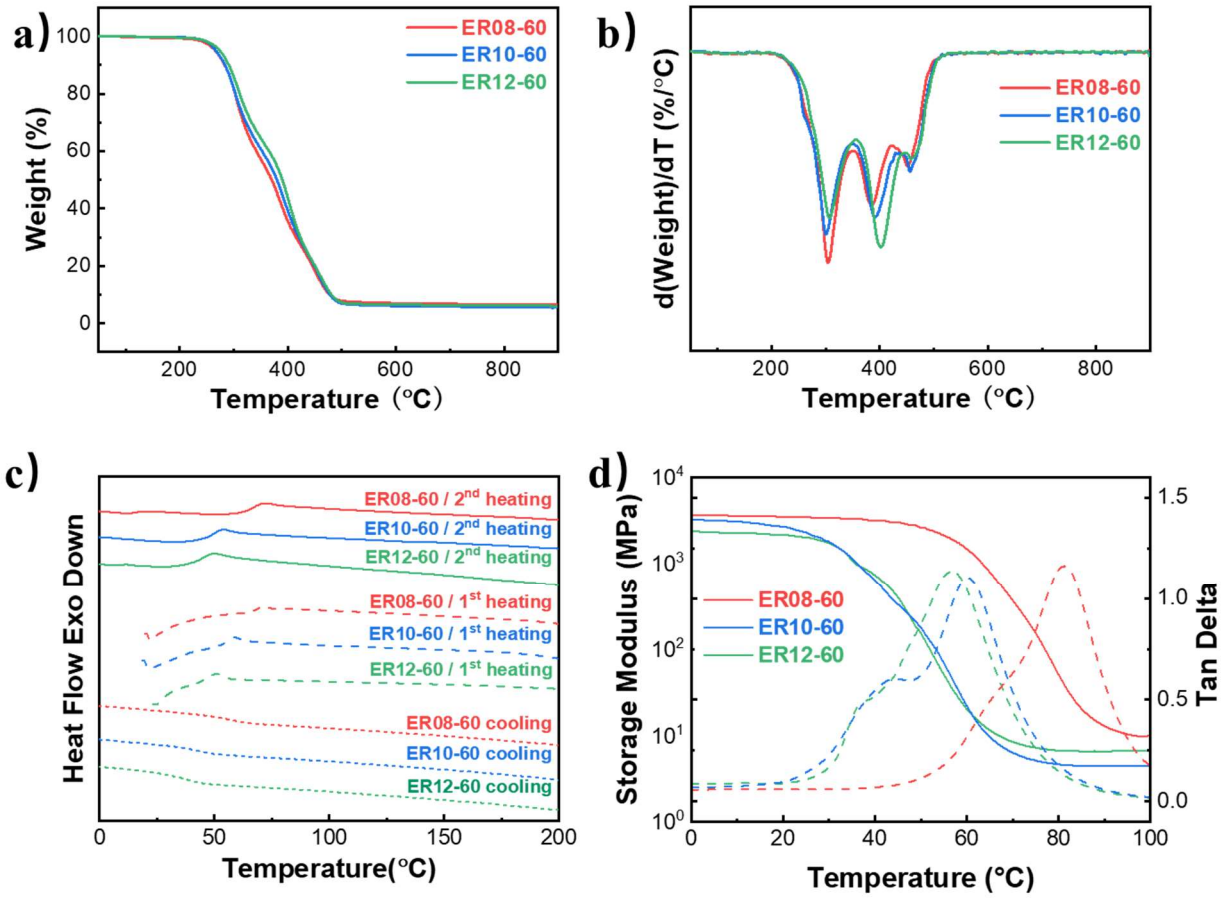

Figure 2. (**a**) TGA curves; (**b**) DTG curves; (**c**) DSC traces and (**d**) DMA curves of the obtained ERs.

The flame retardancy of the ERs was investigated by UL-94 vertical burning test and limit oxygen index (LOI) examination, and the results were listed in Table S1. As we can see from Figure 3a, it took 29 s for ER12-60 to self-extinguish after the first ignition but the self-extinguishing time decreased to 15 s in the recombustion. The UL-94 rating for ER12-60 achieved V-1, with droplets produced throughout the test not igniting the cotton below. The limited oxygen index (LOI) value for ER12-60 was measured to be 23.5%. The flame retardancy performance of ER12-60 was similar to that of ER12-60. The UL-94 rating for ER10-60 also achieved V-1 while the value of LOI was determined to be 24.6%. When comparing the flame retardancy of ER10-60 with ER10-70 and ER10-50, it can be found that the best choice is still ER10-60, which has been confirmed above in the ER12 series. ER08-60 exhibited improved flame retardancy, with a UL-94 rating at V-0 and a LOI value at 27.6% (>27%, nonflammable). Impressively, as shown in Figure 3c, ER08-60 can self-extinguish instantly (<1 s) after the removal of igniter, without melt-dripping. Compared with ER10-70 and ER12-70, the flame retardancy of ER08-70 was slightly weakened, but still reached V-0 rating in the UL-94 vertical burning test. ER08-50 performed much lower flame retardancy as the feed ratio of [COOH]/[epoxy] decreased to 0.5.

Cone calorimeter test offers a simulation of fire conditions and it is usually applied in the analysis of the flame retardancy and combustion behaviors of polymer materials. Heat release rate (HRR) and total heat release (THR) are normally taken directly to refer to the flame retardancy. The HRR and THR curve of the obtained ERs are shown in Figure 4a and 4b, respectively, while the relevant data are listed in the Table 3. ER12-60 had an intense exotherm, and the pHRR and THR reached 602.63 kW/m^2 and 38.11 MJ/m^2, respectively, which is much less than those of traditional $ER_{DGEBA\text{-}DDM}$ (pHRR = 853.99 kW/m^2, THR = 133.52 MJ/m^2) [5]. When the chain length of DAs reduced, the pHRR and THR values reduced further to 349.66 kW/m^2 and 31.98 MJ/m^2 for ER08-60. The results indicated that our ERs have relatively low heat transfer during combustion to exhibit excellent flame retardancy. Practically in fires, most of the victims died from asphyxiation, so it is necessary to assess the smoke emissions and gases production of the obtained ERs. As can be seen in Table 3 and Figure S3, the smoke produce rate (SPR) and the total smoke product (TSP) of all ERs were at a low level. Notably, CO_2 production (see Figure 4c) was high (0.18–0.27 g/s) for all three samples, while the CO production (see Figure4d) was as low as 1.8 mg/s. The results indicated that these ERs have limited fire hazard.

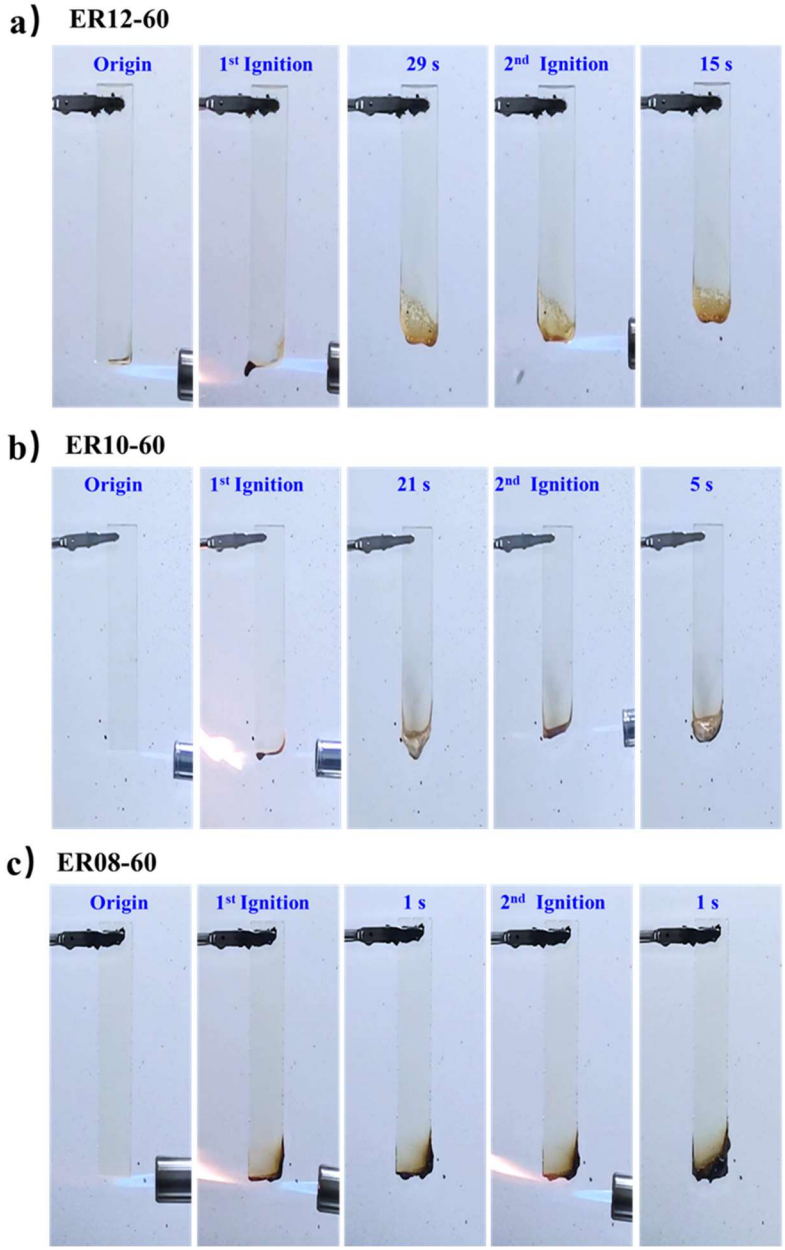

Figure 3. The video screenshots of samples (**a**) ER12-60; (**b**) ER10-60 and (**c**) ER08-60 during vertical burning (UL-94) tests.

The morphology and the chemical structure of the residual coke after combustion could help for understanding the mechanism in the condensed phase. The SEM images of the ER08-60 residual coke collected after UL-94 test and cone calorimetry test are shown in the Figure 5. After UL-94 test, the coke surface of ER08-60 (see Figure 5a) exhibited smooth expansion and the expanded residual carbon surface was distributed with small bumps, which should be caused by the large amount of gas produced during the combustion process. The expanded residual carbon performed as a 'barrier' to protect the substrate from heat and flammable free radicals and therefore combustion is restrained. A complete obturator carbon layer could be observed and many granular protrusions were distributed on the surface of the ER08-60 coke after cone calorimetry test (see Figure 5b). These protrusions were all bubbles. The indications above revealed that ER08-60 produces gas during combustion and the residual coke has the ability to inhibit combustible volatiles, significantly acting as a "barrier" to isolate the substrate from the fire.

Table 3. The data collected from cone calorimetry tests for the obtained ERs.

Sample	TTI (s)	pHRR (kW/m^2)	THR (MJ/m^2)	pSPR (m^2/s)	TSP (m^2)	CO_2P (g/s)	COP (g/s)
ER12-60	21	602.63	38.11	0.039	2.09	0.27	3.4×10^{-3}
ER10-60	19	404.78	34.45	0.023	1.96	0.20	1.9×10^{-3}
ER08-60	21	349.66	31.98	0.024	1.87	0.18	1.8×10^{-3}

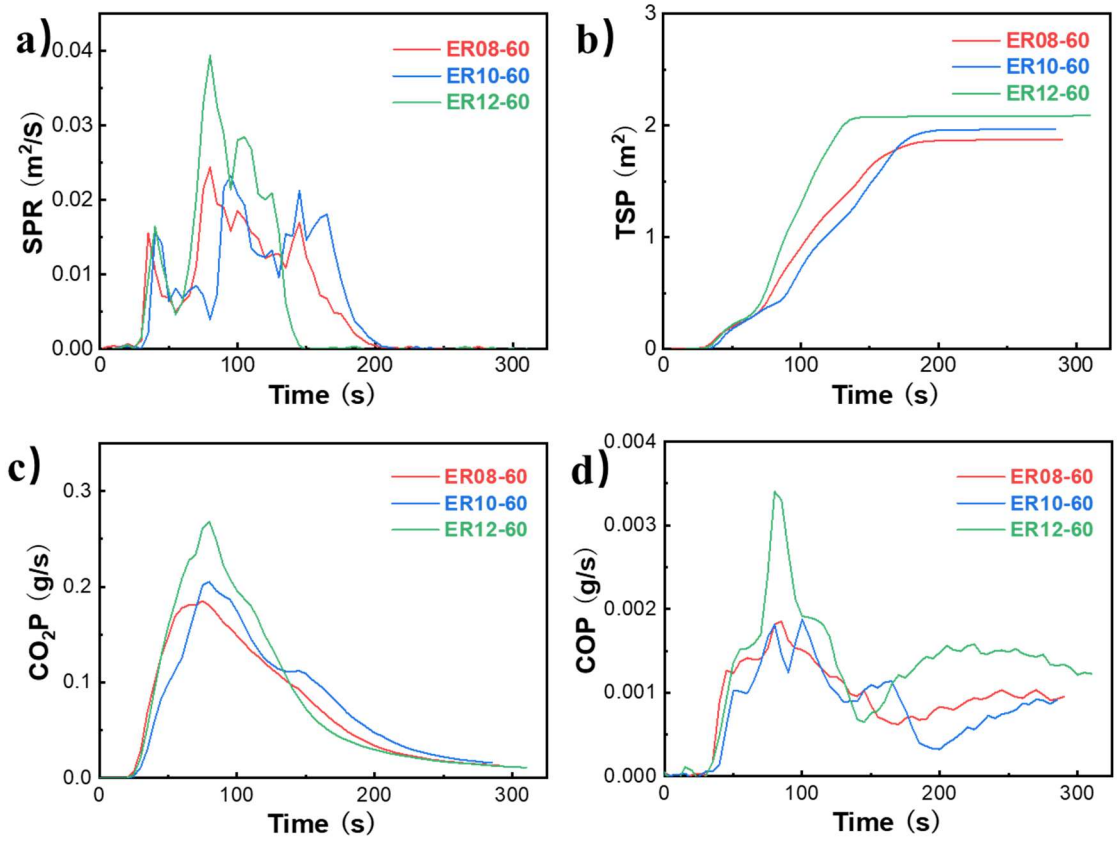

Figure 4. (**a**) HRR; (**b**) THR; (**c**) CO_2P and (**d**) COP curves of ERs recorded by cone calorimetry test.

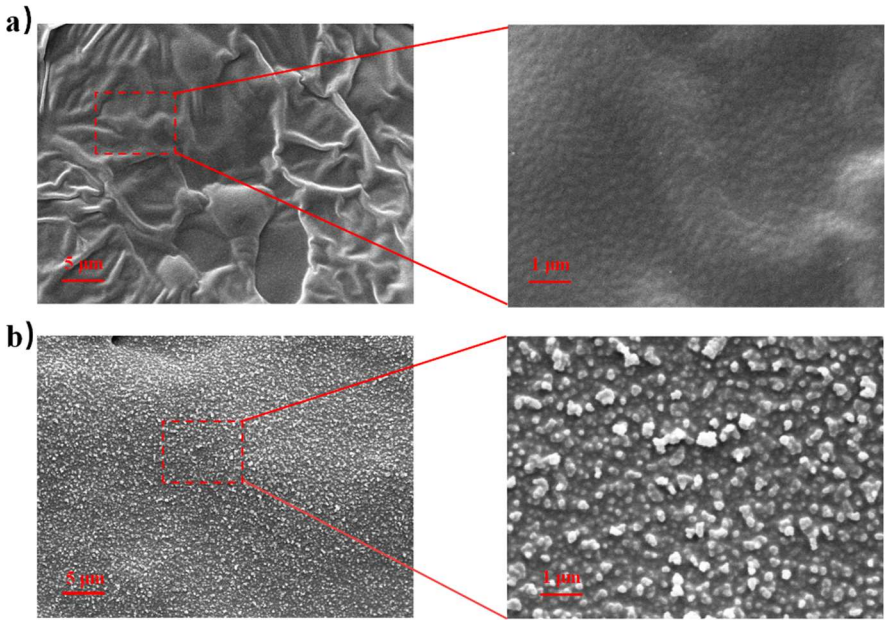

Figure 5. SEM images of the ER08-60 residual coke collected from (**a**) UL-94 test and (**b**) cone calorimetry test.

The chemical composition and state of ER08-60 coke residue after UL-94 test were further analyzed by XPS [11,16,20]. As shown in Figure 6a, elements of C and O can be obviously observed while N element exists in tiny signal. Aromatic carbon, aliphatic C–C and C–H, C–N, C–O–C, C–OH and O–C=O can be found (see Figure 6b). Pyridine nitrogen is thought to be more stable on heat than pyrrole nitrogen and it benefits for the forming of a more stable carbon layer (see Figure S4). All the results indicated that ER08-60 is able to form more aromatized C–C and C–N crosslinked coke upon combustion and in this case, the performance of self-extinguishing and flame retarding can be improved.

The gas phase product of ER08-60 was analyzed by TG-IR, and the 3D spectrum is shown in Figure 6c. All volatile pyrolysis products can be distinguished by their typical peak ranges [4]. The band appears at 3400–4000 cm^{-1} attributed to the absorption vibration peak of H_2O and the highest absorption peak at 2450 cm^{-1} indicates the release of CO_2. The peak at 2950–2915 cm^{-1}

belongs to the symmetric and asymmetric vibration of aliphatic olefin. The peaks of carbonyl compounds relate to 1850–1650 cm^{-1}. The band at 1550–1300 cm^{-1} can be attributed to the vibration peak of aromatic compounds, while that at 970–900 cm^{-1} belongs to the vibration peak of NH_3. It is interesting to see from Figure 6d that the decomposition process of ER08-60 is mainly divided into three stages. In the first stage at 300 °C, CO_2, NH_3 and H_2O are found to release, which can be attributed to the decomposition of isocyanurate ring. At 375 °C, the compounds released are mainly CO_2 and carbonyl compounds (such as aliphatic ester or acid), along with aromatic compounds and a small amount of NH_3. When the temperature reaches as high as 450 °C, further decomposition takes place to release CO_2. The release of CO_2 can be observed at each stage of the decomposition of ER08-60. Thus, the oxygen surrounding is excluded in the system and the combustion is inhibited.

The tensile curves of ERs are shown in Figure S5 while the results of the tensile and bending tests are summarized in Table 4. The tensile and bending properties of the obtained ERs improved with the decrease of the chain length of DAs. For ER08-60, the tensile stress at break (σ_b), the Young's modulus (E), the bending strength (σ_t), the bending modulus (E_f) and the elongation at break (ε_t) were 86.6 MPa, 1628 MPa, 75.4 MPa, 1711 MPa and 22%, respectively. The values of σ_b for ER10-60 and ER12-60 decreased to 62.3 and 32.4 MPa, respectively.

The crosslinking density of ERs can also be calculated from the tensile curves, via Equation (1) [32,33].

$$E = 3V_eRT \tag{1}$$

where E is the Young's modulus detected from tensile test, T is the absolute temperature for tensile test, R is the ideal gas constant (8.314 J/mol K), V_e is the crosslinking density.

V_e values calculated via Eq. (1) are listed in Table 4 and we can see that the crosslinking density increases with the decline of chain length of DAs. As a result, the tensile and bending strength increases accordingly. The rigid isocyanurate structure offers the stiffness while the long methylene structure offers the flexibility, which provides proper mechanical properties for the final products.

Table 4. The mechanical properties of ERs.

Sample	E (MPa)	V_e (mol/m^3)	σ_b (MPa)	ε_b (%)	E_f (MPa)	σ_t (MPa)
ER12-60	683±38	918±52	32.4±0.8	122±11	161±8	10.7±0.5
ER10-60	909±41	1254±56	62.3±2.7	72±6	695±8	33.0±0.3
ER08-60	1628±74	2189±100	86.6±2.8	22±2	1711±14	75.4±1.2

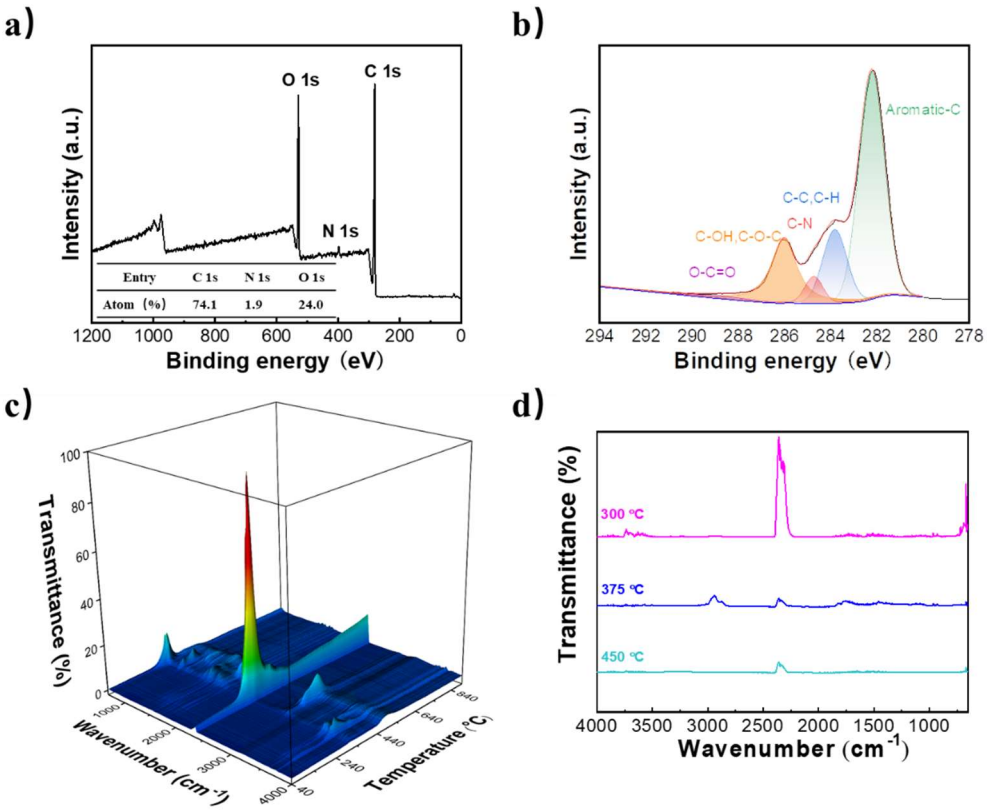

Figure 6. (**a**)Wide-scan XPS spectrum; (**b**) C1s XPS spectrum of ER08-60 coke residue; (**c**) 3D TG-IR spectra of the degradation component in gas phase; and (**d**) FT-IR spectra of the pyrolysis for ER08-60.

As it can be seen from Scheme 1 that the backbone of in the obtained ER networks are mainly polyester. Therefore, the products should be hydrolysable, in both acidic and alkaline solutions. ER12-60, ER10-60 and ER08-60 were immersed in water, hydrochloric acid and sodium hydroxide solution with different concentrations. As shown in the Figure 7, ER08-60 could neither decompose nor swell in water for 5 d. However, it broke down into fragments when soaking in hydrochloric acid solution, and the degradation went faster with the increase of hydrochloric acid concentration. Soaked in 1, 2 and 4 mol/L sodium hydroxide solution, ER08-60 degraded within 1 day. The decomposition products dissolved in the solution so that a clear solution could be observed. When the concentration of the solution is further increased to 8 mol/L, it is found that the degradation of this material is not satisfactory. In Figure S6, the ^{1}H NMR spectra of solution and solid product have proved that DA08 is the insoluble substance and its content in the solid product is more than that in the solution. It is further understandable since the solubility of DA08 in 8 mol/L NaOH solution is poor (see Fig S7).

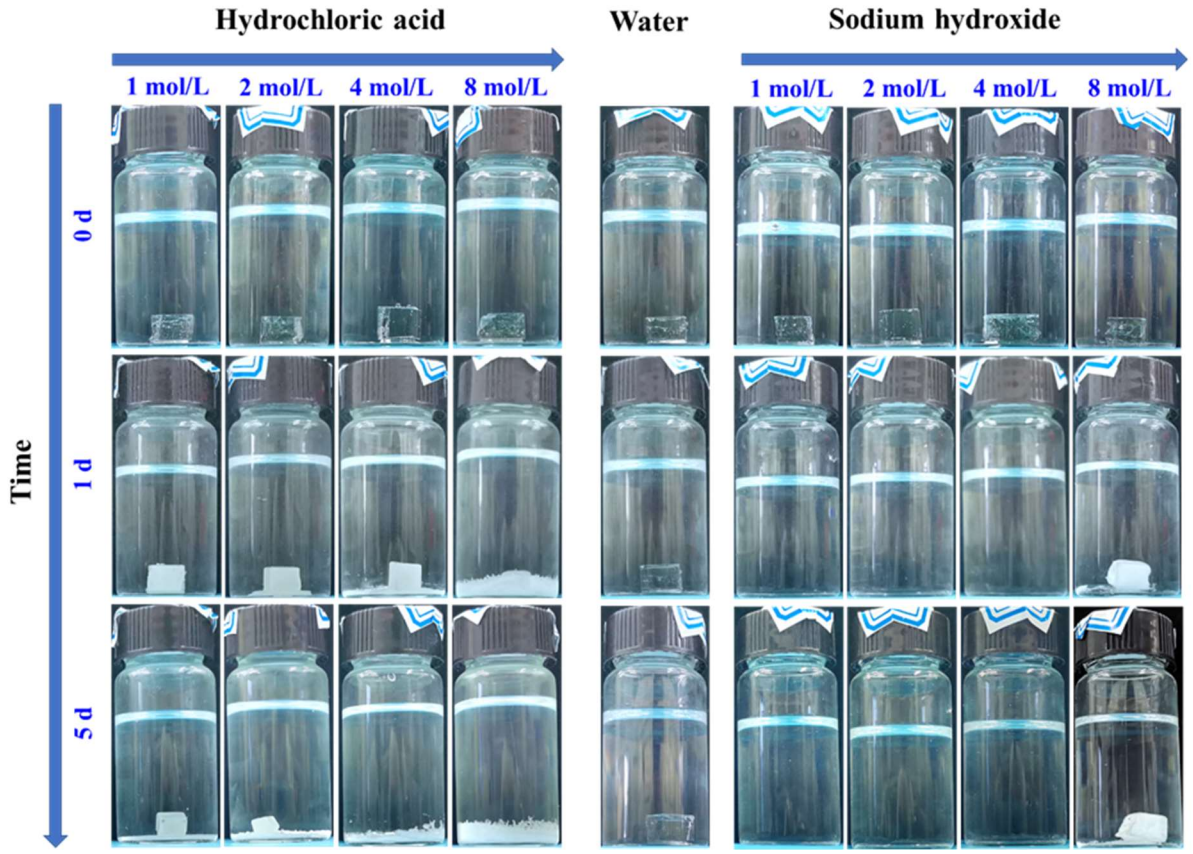

Figure 7. Photo images of ER08-60 hydrolyzation samples in acidic, neutral and basic solutions.

When ER08-60 degrades from the surface, the degradation product DA08 releases and covers on the surface of the bulk, which prevents further permeation of NaOH solution into the bulk. The high concentration of sodium hydroxide may prevent the dissolution of the decomposition products. The hydrolysis of ER12-60 and ER10-60 performs similar to that of ER08-60 (see Figure S8).

4. Conclusions

Transparent and hydrolysable ERs with intrinsic flame retardancy were prepared by melting polymerization of TGIC with DAs, without using catalysts. A feed ratio of [COOH]/[epoxy] at 0.6 was found to be good for the reaction since transesterification takes place during the curing process so that the content of COOH can be less. ER08-60 exhibited excellent flame retardancy, with a UL-94 rating at V-0 and a value of LOI at 27.6%. The flame retardancy of ER10-60 (V-1 and LOI 24.6%) and ER12-60 (V-1 and LOI 23.5%) was not as good as ER08-60. Our study revealed that isocyanurate ring decomposes first and CO_2 releases during combustion, which prevents the contact of oxygen. Since the isocyanurate content in ER08-60 is higher than that in ER10-60 or ER12-60, it is understandable that the flame retardancy of ER08-60 is the best. The mechanical and degradation properties of these ERs are also found to be good. The transparency of these materials was tested to be around 85%. This study provides a way for the development of more economical and environmentally friendly flame retarded materials.

Supplementary Materials

The following supporting information can be found at: https://www.sciepublish.com/index/journals/article/spe/30/id/47. Fig. S1: UV-vis spectra and the appearance of the obtained ERs; Fig. S2: Photo images of ER12-100/80/60 (a) before and (b) during UL-94 tests; Fig. S3: The (a) SPR and (b) TSP curves in cone calorimetry tests for the obtained ERs; Fig. S4: N1s XPS spectra of ER08-60; Fig. S5: The tensile test curve of the obtained ERs; Fig. S6: Photo images of (a) ER10-60 and (b) ER12-60 hydrolyzation samples in acidic, neutral and basic solutions.

Author Contributions

Conceptualization, D. Tang and T. Ma; Methodology, D. Tang and T. Ma; Validation, D. Tang and T. Ma; Formal Analysis, D. Tang and T. Ma; Investigation, D. Tang; Resources, D. Tang; Data Curation, D. Tang; Writing – Original Draft Preparation, T. Ma; Writing – Review & Editing, D. Tang; Supervision, D. Tang; Project Administration, D. Tang; Funding Acquisition, D. Tang.

Ethics Statement

Not applicable.

Informed Consent Statement

Not applicable.

Funding

This research was funded by National Natural Science Foundation of China (No. 21404040, 21734004), and the Fund of Guangdong Provincial Key Laboratory of Luminescence from Molecular Aggregates (South China University of Technology, No. 2019B030301003).

Declaration of Competing Interest

The authors declare that they have no known competing financial interests or personal relationships that could have appeared to influence the work reported in this paper.

References

1. Auvergne R, Caillol S, David G, Boutevin B, Pascault JP. Biobased thermosetting epoxy: present and future. *Chem. Rev.* **2014**, *114*, 1082–115.
2. Domun N, Hadavinia H, Zhang T, Sainsbury T, Liaghat GH, Vahid S. Improving the fracture toughness and the strength of epoxy using nanomaterials-a review of the current status. *Nanoscale* **2015**, *7*, 10294–10329. https://doi.org/10.1039/c5nr01354b.
3. Chen L, Chai S, Liu K, Ning N, Gao J, Liu Q, et al. Enhanced epoxy/silica composites mechanical properties by introducing graphene oxide to the interface. *ACS Appl. Mater. Interfaces* **2012**, *4*, 4398–4404. https://doi.org/10.1021/am3010576.
4. Zhang W, Huang J, Guo X, Zhang W, Qian L, Qin Z. Double organic groups-containing polyhedral oligomeric silsesquioxane filled epoxy with enhanced fire safety. *J. Appl. Polym. Sci.* **2022**, *139*, e52461. https://doi.org/10.1002/app.52461.
5. Yang Q, Jia Y, Zhou X, Zhang H. Mechanically reinforced flame-retardant epoxy resins by layered double hydroxide in situ decorated carbon nanotubes. *ACS Appl. Polym. Mater.* **2022**, *4*, 6731–6741. https://doi.org/10.1021/acsapm.2c01110.
6. Wan J, Zhao J, Zhang X, Fan H, Zhang J, Hu D, et al. Epoxy thermosets and materials derived from bio-based monomeric phenols: Transformations and performances. *Prog. Polym. Sci.* **2020**, *108*, 101287. https://doi.org/10.1016/j.progpolymsci.2020.101287.
7. Wang X, Guo W, Song L, Hu Y. Intrinsically flame retardant bio-based epoxy thermosets: A review. *Compos. Part B Eng.* **2019**, *179*, 107487.
8. Rad ER, Vahabi H, de Anda AR, Saeb MR, Thomas S. Bio-epoxy resins with inherent flame retardancy. *Prog. Org. Coat.* **2019**, *135*, 608–612.
9. Kamjornsupamitr T, Hunt AJ, Supanchaiyamat N. Development of hyperbranched crosslinkers from bio-derived platform molecules for the synthesis of epoxidised soybean oil based thermosets. *RSC Adv.* **2018**, *8*, 37267–37276. https://doi.org/10.1039/c8ra07133k.
10. Tellers J, Willems P, Tjeerdsma B, Guigo N, Sbirrazzuoli N. Eutectic hardener from food-based chemicals to obtain fully bio-based and durable thermosets. *Green Chem.* **2020**, *22*, 3104–3110. https://doi.org/10.1039/d0gc00311e.
11. Lu Y, Zhang Y, Zhang K. Renewable biomass resources to access halogen- and phosphorus-free flame retardant thermosets with ultra-low heat release capacity. *Chem. Eng. J.* **2022**, *448*, 137670. https://doi.org/10.1016/j.cej.2022.137670.
12. Bhakare MA, Lokhande KD, Bondarde MP, Dhumal PS, Some S. Dual functions of bioinspired, water-based, reusable composite as a highly efficient flame retardant and strong adhesive. *Chem. Eng. J.* **2023**, *454*, 140421.
13. Ménard R, Negrell C, Fache M, Ferry L, Sonnier R, David G. From a bio-based phosphorus-containing epoxy monomer to fully bio-based flame-retardant thermosets. *RSC Adv.* **2015**, *5*, 70856–70867. https://doi.org/10.1039/c5ra12859e.
14. Wu Q, Xiao L, Chen J, Peng Z. Facile fabrication of high-performance epoxy systems with superior mechanical properties, flame retardancy, and smoke suppression. *J. Appl. Polym. Sci.* **2022**, *140*, e53480. https://doi.org/10.1002/app.53480.

15. Wang S, Ma S, Xu C, Liu Y, Dai J, Wang Z, et al. Vanillin-derived high-performance flame retardant epoxy resins: facile synthesis and properties. *Macromolecules* **2017**, *50*, 1892–1901. https://doi.org/10.1021/acs.macromol.7b00097.
16. Qi Y, Weng Z, Kou Y, Song L, Li J, Wang J, et al. Synthesize and introduce bio-based aromatic s-triazine in epoxy resin: enabling extremely high thermal stability, mechanical properties, and flame retardancy to achieve high-performance sustainable polymers. *Chem. Eng. J.* **2021**, *406*, 126881. https://doi.org/10.1016/j.cej.2020.126881.
17. Shao Z, Wang H, Li M, Chen T, Xu Y, Yuan C, et al. Effect of functionalized graphene oxide with phosphaphenanthrene and isocyanurate on flammability, mechanical properties, and thermal stability of epoxy composites. *J. Appl. Polym. Sci.* **2019**, *137*, 48761.
18. Hou R, Zhang Z, Zhang G, Tang D. Synthesis and properties of thermoplastic polyisocyanurates: polyisocyanuratoamide, polyisocyanurato(ester-amide) and polyisocyanurato(urea-ester). *J. Renew. Mater.* **2020**, *8*, 397–403.
19. Chen Z, Hou R, Cheng J, Fang F, Tang D, Zhang G. Polyisocyanuratoesters: renewable linear polyesters with high flame retardancy. *J. Renew. Mater.* **2018**, *6*, 584–590. https://doi.org/10.32604/jrm.2018.00120.
20. Hou B, Zhang W, Lu H, Song K, Geng Z, Ye X, et al. Multielement Flame-Retardant System Constructed with Metal POSS-Organic Frameworks for Epoxy Resin. *ACS Appl. Mater. Interfaces* **2022**, *14*, 49326–49337 https://doi.org/10.1021/acsami.2c14740.
21. Yuan ZG, Shu ZH, Qi L, Cai WA, Liu WB, Wang J, et al. Curing behavior, mechanical, and flame-retardant properties of epoxy-based composites filled by expandable graphite and ammonium polyphosphate. *J. Appl. Polymer Sci.* **2022**, *140*, e53267.
22. Qi Y, Weng Z, Zhang K, Wang J, Zhang S, Liu C, et al. Magnolol-based bio-epoxy resin with acceptable glass transition temperature, processability and flame retardancy. *Chem. Eng. J.* **2020**, *387*, 124115. https://doi.org/10.1016/j.cej.2020.124115.
23. Liu G, Gao S. Synergistic effect between aluminum hypophosphite and a new intumescent flame retardant system in poly(lactic acid). *J. Appl. Polymer Sci.* **2018**, *135*, 46359. https://doi.org/10.1002/app.46359.
24. Wang X, Hu Y, Song L, Xing W, Lu H. Preparation, flame retardancy, and thermal degradation of epoxy thermosets modified with phosphorous/nitrogen-containing glycidyl derivative. *Polymers Adv. Technol.* **2012**, *23*, 190–197. https://doi.org/10.1002/pat.1851.
25. Wu K, Kandola BK, Kandare E, Hu Y. Flame retardant effect of polyhedral oligomeric silsesquioxane and triglycidyl isocyanurate on glass fibre-reinforced epoxy composites. *Polymer Composites* **2011**, *32*, 378–389. https://doi.org/10.1002/pc.21052.
26. Abdullayev Y, Javadova V, Valiyev I, Talybov A, Salmanov C, Autschbach J. Ionic Liquid-Mediated Urea Pyrolysis to Cyanuric Acid: Experimental Protocol and Mechanistic Insights. *Ind. Eng. Chem. Res.* **2022**, *61*, 15076–15084. https://doi.org/10.1021/acs.iecr.2c02791.
27. Ding C, Shuttleworth PS, Makin S, Clark JH, Matharu AS. New insights into the curing of epoxidized linseed oil with dicarboxylic acids. *Green Chem.* **2015**, *17*, 4000–4008. https://doi.org/10.1039/c5gc00912j.
28. Liu H, Wu X, Liu Y, Guo Z, Ge Q, Sun Z. The curing characteristics and properties of bisphenol A epoxy resin/maleopimaric acid curing system. *J. Mater. Res. Technol.* **2022**, *21*, 1655–1665. https://doi.org/10.1016/j.jmrt.2022.10.008.
29. Schwaiger M, Resch-Fauster K. Mechanical flexible epoxy resins with 100% bio-based carbon content based on epoxidized vegetable oils. *J. Appl. Polymer Sci.* **2022**, *139*, e53233.
30. Li A, Li K. Pressure-Sensitive Adhesives Based on Epoxidized Soybean Oil and Dicarboxylic Acids. *ACS Sustain. Chem. Eng.* **2014**, *2*, 2090–2096. https://doi.org/10.1021/sc5003853.
31. Li S, Ren J, Yuan H, Yu T, Yuan W. Influence of ammonium polyphosphate on the flame retardancy and mechanical properties of ramie fiber-reinforced poly(lactic acid) biocomposites. *Polymer Int.* **2010**, *59*, 242–248. https://doi.org/10.1002/pi.2715.
32. Eroğlu M. Characterization of the network structure of hydroxyl terminated poly(butadiene) elastomers prepared by different reactive systems. *J. Appl. Polymer Sci.* **1998**, *70*, 1129–1135.
33. Aprem A, Joseph K, Thomas S. Studies on double networks in natural rubber vulcanizates. *J. Appl. Polymer Sci.* **2004**, *91*, 1068–1076.